

Fast and Reliable Transient Simulation and Continuous Optimization of Large-Scale Gas Networks

Pia Domschke

Frankfurt School of Finance & Management, Finance Department,
Adickesallee 32-34, 60322 Frankfurt am Main, Germany
p.domschke@fs.de

Oliver Kolb

University of Mannheim, Department of Mathematics,
A5, 6, 68131 Mannheim, Germany
kolb@uni-mannheim.de

Jens Lang*

Technical University of Darmstadt, Department of Mathematics,
Dolivostraße 15, 64293 Darmstadt, Germany
lang@mathematik.tu-darmstadt.de

November 8, 2021

Abstract

We are concerned with the simulation and optimization of large-scale gas pipeline systems in an error-controlled environment. The gas flow dynamics is locally approximated by sufficiently accurate physical models taken from a hierarchy of decreasing complexity and varying over time. Feasible work regions of compressor stations consisting of several turbo compressors are included by semiconvex approximations of aggregated characteristic fields. A discrete adjoint approach within a first-discretize-then-optimize strategy is proposed and a sequential quadratic programming with an active set strategy is applied to solve the nonlinear constrained optimization problems resulting from a validation of nominations. The method proposed here accelerates the computation of near-term forecasts of sudden changes in the gas management and allows for an economic control of intra-day gas flow schedules in large networks. Case studies for real gas pipeline systems show the remarkable performance of the new method.

Keywords: transient gas supply networks, model hierarchy, error estimators, adaptivity, optimal control

AMS subject classifications: 65K99, 65Z99, 65M22, 35Q93

*corresponding author, ORCID: 0000-0003-4603-6554

1 Introduction

The ongoing replacement of traditional energy production by coal fired and nuclear plants with gas consuming facilities has rapidly increased the role of natural gas transport through large networks. The security of energy supply and the development of clean energy to meet environmental demands have generated a significant increase in gas consumption for electric power stations in the last decade. In these days, natural gas is considered as a bridging combustible resource on the way towards a future energy mix mainly based on low-carbon and regenerative energy [18]. The seasonally fluctuating disposability of wind and solar resources causes a growing variability in electricity production and hence also in the demands of gas transportation by pipelines. The resulting intra-day oscillations in demand for natural gas leads to new challenges for computer based modelling and control of gas pipeline operations with an increasing focus on short-term transient dynamics of gas flow. Operators have to responsively control loads to realize a reliable operational management for both gas and electricity delivery systems. The challenging new conditions demand advanced decision tools based on transient nonlinear optimization taking into account serious operating restrictions.

In this paper, we propose a novel computational approach for the reliable transient simulation and continuous optimization for gas pipeline flow through networks. The operation of compressor stations and flow schedules are determined in such a way that operating limits of compressors and pressure constraints inside the pipes are satisfied. Exemplarily, we investigate the important task of safely driving a stationary running system from an initial condition to a target state defined by shifted gas nominations at the entrances or delivery points of the network. To be usable in real-time gas management, we have designed our methods to meet user-defined accuracies while keeping the computing time for large-scale gas networks at a moderate level. The proposed method is fast enough to allow the application of uncertainty quantification by Monte Carlo or other stochastic simulations for risk analysis and reliability assessment of gas delivery.

The highly nonlinear partial differential equations representing the constraints of gas flow dynamics are locally approximated by a certain flow model taken from a whole hierarchy of decreasing complexity. Error estimates are computed from sensitivity equations and used as the basis for a straightforward criterion to verify that the model chosen provides a physically meaningful representation of the local gas flow in a pipe. Similar estimators are exploited to set up a fully adaptive spatial resolution in each individual pipe and variable time steps in a finite volume setting, which greatly reduces the size of the resulting discretized system. These strategies have been already proven to work reliably for networks of academic size [4, 8].

Multiple compressor stations consisting of several compressor machines often connected through intricate topological designs compensate the pressure drop due to the inherent friction or user's excessive withdrawal of natural gas. Additionally, complex constraint envelopes delimit the allowed operating states of the compressors, making a generalized modelling and managing of such stations a challenging task of its own. To enable an efficient usage within a nonlinear optimization, we extend the approximate convex decomposition developed in [17, 26] to a semiconvex setting. Critically, a semiconvex approximation of the characteristic work diagram for a compressor station enables a new representation of compressor constraints and can be used for a fast validation of nominations.

The development of an optimization-based, automated decision system requires the cal-

ulation of gradient information to be completed repeatedly and reliably in a short time in order to provide a decision support that is usable in a real-time gas management for large-scale pipeline systems. We propose to use a discrete adjoint approach within a first-discretize-then-optimize strategy applied to a possible splitting of the overall time horizon into smaller subintervals. A sequential quadratic programming with an active set strategy is then applied to solve the resulting nonlinear constrained optimization problems [33, 34].

There are many academic and industrial studies available in the literature for the gas transport through a single pipe or even whole gas networks. In the last fifteen years, an increasing effort for the optimization of transient processes has led to a couple of publications that consider gas pipeline systems of moderate size [2, 5, 8, 11, 15, 16, 28, 30]. Very recently, a linearization procedure that enables the use of closed-form solutions for the gas transport equations was proposed in [1] and applied to middle-sized networks. Significant progress has been made in developing sophisticated models for compressor stations, which is a key for more realistic treatment of an adjusted pressure increase under certain operating limits [1, 31, 35]. The gas flow in larger pipeline systems may be regulated by control valves and groups of compressors could be inactive in certain time intervals. Optimization of such systems leads to transient mixed-integer nonlinear problems. Although significant progress has been made to tackle these challenging problems in recent years, they still remain unsolved for real-life applications with sudden changes in gas supply and demand, which requires detailed transport models and reliable numerical solutions [2, 5, 14, 27]. Model order reduction is an appropriate technique to reduce the computational cost for simulating large-scale gas networks. Surrogates based on radial functions and proper orthogonal decomposition for quasi-static approximations of the gas flow are compared in [12]. However, the construction of such models in the case of highly transient flow with nonlinear compressors is still very ambitious. Recently, the tracking of internal space-time flow and pressure profiles using pressure measurements at nodal junctions and optimization-based state estimates has been investigated in [20] for simplified compressor models and networks of moderate size. Graph-based modeling abstractions with application to optimal control of connected gas pipelines in series is proposed in [19]. The challenging task of maximizing the economic welfare of gas users for slow transients that allow a simplification of Euler’s equations is the objective in [36]. To the best of our knowledge, in all these approaches there is no rigorous control of the discretization errors caused by the space-time resolution and model selection.

We apply our novel computation and optimization approach to real networks taken from the GasLib library [32]. Fully model-space-time-adaptive simulations provide accuracy bounds for target functionals and can be viewed as an efficient way to automatically and safely reduce the order of the gas network model. They can be computed in the range of seconds for several hundreds of edges including pipes, valves, and compressor stations. Making use of this acceleration and calling the simulation tool within a nonlinear continuous optimization solver to determine gradient information reduces the computing time to validate nominations by several orders of magnitude compared to previously developed methods. The approach may be promising to include binary decision variables and to perform reliability studies using methods from uncertainty quantification in future extensions.

The paper is structured as follows. In Section 2, we outline our gas network modelling including boundary and coupling conditions, modelling of gas flow through pipes, compressor stations, and valves. Our numerical schemes for simulation and optimization are described in Section 3. In Section 4 and 5, we present results for certain case studies including nomination validation. Finally, a short summary and a outlook are given in Section 6.

2 Gas Network Modelling

We model gas supply networks as a directed graph $\mathcal{G} = (\mathcal{J}, \mathcal{V})$ with arcs \mathcal{J} and vertices \mathcal{V} (nodes, branching points). The set of arcs \mathcal{J} contains pipes, compressor stations, simple valves and control valves. The gas dynamics within the pipes is described by a hierarchy of models of different complexity ranging from simple algebraic equations to a hyperbolic system of PDEs (see below and compare to [8]). For each arc in the network that is modelled by a PDE, we consider an interval $[x_j^a, x_j^b]$ with $x_j^a < x_j^b$, $j \in \mathcal{J}_{\text{PDE}}$, where $\mathcal{J}_{\text{PDE}} \subseteq \mathcal{J}$ contains all arcs modelled with PDEs. All other network components, including coupling and boundary conditions at the nodes, are described by algebraic equations, where we also use spatial coordinates x_j^a and x_j^b to describe states at the beginning (tail) and end (head) of an arc $j \in \mathcal{J} \setminus \mathcal{J}_{\text{PDE}}$ or denote states at the beginning/end of the arc with subscripts “in”/“out”. Note that one has to specify adequate initial, coupling and boundary conditions for a complete problem description of the gas network.

The flow through the network is described by the state variables $q(x, t)$ and $p(x, t)$. Here, q denotes the flow rate (or flux) in m^3/s under standard conditions, i.e., pressure of 1 atm and temperature of $0^\circ\text{C} = 273.15\text{ K}$, and p represents the pressure in Pa.

Coupling and Boundary Conditions. For any node $v \in \mathcal{V}$, we denote by δ_v^- the ingoing arcs of v and the outgoing arcs by δ_v^+ . Respecting conservation of mass, the entire flux going into any node has to be equal to the sum of fluxes going out of that node:

$$\sum_{j \in \delta_v^+} q(x_j^a, t) - \sum_{j \in \delta_v^-} q(x_j^b, t) = q(v, t) \quad \forall t > 0 \quad (1)$$

where $q(v, t)$ is an auxiliary variable to model the flow rate of a feed-in or demand at node v (see below). Otherwise, it is set to zero. In addition to conservation of mass, it is widely used to claim the equality of pressure at all nodes $v \in \mathcal{V}$, that is,

$$p(x_j^a, t) = p(v, t) \quad \forall j \in \delta_v^+, \quad p(x_i^b, t) = p(v, t) \quad \forall i \in \delta_v^-, \quad (2)$$

with an auxiliary variable $p(v, t)$ for the pressure at the node v . For coupling and boundary nodes, one has to pose one more condition, which we consider of the form

$$e(p(v, t), q(v, t)) = 0. \quad (3)$$

The latter allows for prescribing pressure or flux profiles as boundary condition or feed-in/demand. For example, the pressure is often described at the inflow boundary and certain flux profiles are requested by the gas consumers at the outflow boundary. Other coupling conditions like conservation of energy or entropy for isothermal, isentropic or polytropic gas flow, respectively, are discussed in [10, 25, 29].

Modelling of Gas Flow through Pipes. Typically, gas pipeline systems are buried underground and hence temperature differences between a pipe segment and the ground can be neglected in practice. It is therefore standard to consider an isothermal process without a conservation law for the energy. As most complex model for the gas dynamics in the pipes, we take

- (M3), the scaled isothermal Euler equations

$$u_t + (\mathbf{A}u + B(u))_x = g(u), \quad (4)$$

with

$$u = \begin{pmatrix} p \\ q \end{pmatrix}, \quad \mathbf{A} = \begin{pmatrix} 0 & \frac{\rho_0 c^2}{A} \\ \frac{A}{\rho_0} & 0 \end{pmatrix}, \quad B(u) = \begin{pmatrix} 0 \\ \frac{\rho_0 c^2 q^2}{Ap} \end{pmatrix}, \quad g(u) = \begin{pmatrix} 0 \\ -\frac{\lambda \rho_0 c^2 |q|q}{2dAp} \end{pmatrix},$$

together with the equation of state for real gases, $p = \rho zRT$, with the density ρ , the compressibility factor $z \in (0, 1)$ [22], the temperature T , and the specific gas constant R . Here, $c = \sqrt{p/\rho}$ denotes the speed of sound, λ the friction coefficient, d the diameter, A the cross-sectional area of the pipe, and ρ_0 the density under standard conditions. Neglecting the nonlinear term $B(u)$ on the left hand side leads to

- (M2), the semilinear isothermal Euler equations

$$u_t + \mathbf{A}u_x = g(u). \quad (5)$$

As third and most simplest model, we consider

- (M1), the (quasi-)stationary semilinear isothermal Euler equations

$$\mathbf{A}u_x = g(u), \quad (6)$$

which can be solved analytically,

$$q = \text{const.}, \quad (7a)$$

$$p_{\text{out}} = \sqrt{p_{\text{in}}^2 - \frac{\lambda \rho_0^2 c^2 L}{dA^2} |q|q}. \quad (7b)$$

Here, L denotes the length of the pipe. The flow rate q is now only represented by the pressure difference in a pipe - the so-called Weymouth equation. It is the standard model to capture long-term planning behaviour of gas networks in the quasi-stationary regime.

To summarize, the three models (M3)-(M2)-(M1) forms a hierarchy of gas transport models with decreasing fidelity. For later use, it is important to mention that they are characterized by an additive structure, i.e., they are related by adding or subtracting certain differential terms. Given a reliable accuracy control, they can be used in each individual pipe adopted to the local flow behaviour without any difficulty, since the state vector $u = (p, q)$ remains unchanged and hence two pipes can be easily interconnected by the continuity of p and q .

Modelling of Compressor Stations. Compressor stations consist of at least one turbo compressor, where typically various ways of controlling the entire station are available (parallel, series, subsets). Thus a direct approach of modelling a compressor station leads to mixed integer control problems [31]. As a simplification, an outer linear approximation of the feasible states of a compressor station is proposed in [35]. This results in a characteristic diagram given by a polyhedral model in the (Q, H_{ad}) -space, where $Q = q\rho_0/\rho$ is the volumetric flow rate in m^3/s and H_{ad} is the adiabatic head of the compressor defined by the gas compression from p_{in} to p_{out} :

$$H_{\text{ad}} = zTR_s \frac{\kappa}{\kappa - 1} \left(\left(\frac{p_{\text{out}}}{p_{\text{in}}} \right)^{\frac{\kappa-1}{\kappa}} - 1 \right). \quad (8)$$

Here, κ is the isentropic exponent and $R_s := R/m$ is the specific gas constant with m being the averaged molar mass of the gas mixture.

We make use of such compressor station models to be able to apply methods from continuous nonlinear optimization for optimal control tasks. Therefore, H_{ad} is used as time-dependent control variable, while the underlying polyhedral model is incorporated as state constraint within the optimization procedures. The power P that is needed for the compression process is given by $P = \rho_{\text{in}} Q H_{\text{ad}} / \eta_{\text{ad}}$, where $\eta_{\text{ad}} \in [0, 1]$ denotes the adiabatic efficiency depending on Q , the compressor speed, and other compressor-specific parameters [31, 35]. For later use, we denote by \mathcal{J}_{cp} the set of all compressor stations.

Modelling of Valves. Valves are used to regulate the flow in gas networks. The equations describing an open simple valve are

$$q_{\text{in}} = q_{\text{out}}, \quad p_{\text{in}} = p_{\text{out}}. \quad (9)$$

A closed simple valve is described by $q_{\text{in}} = q_{\text{out}} = 0$. A special class of valves are control valves that reduce the gas pressure by a certain amount. The corresponding equations are given by

$$p_{\text{in}} - p_{\text{out}} = \Delta p, \quad q_{\text{in}} = q_{\text{out}}, \quad (10)$$

with a possibly time-dependent control variable $\Delta p = \Delta p(t)$.

3 Numerical Schemes for Simulation and Optimization

With the different models described above and all controls $(H_{\text{ad}}(t), \Delta p(t))$ given, we can solve the whole network as a system of differential-algebraic equations using adequate initial, coupling, and boundary conditions. Since the gas transport through a complex network may be very dynamic and thus changes both in space and time, an automatic control of the accuracy of the simulation is mandatory. In addition, a model adaptation, i.e., switching between models (M3), (M2), and (M1) in an appropriate way, has proven to be very useful in order to further reduce computational costs. The main idea is to use the most complex model (M3) only when necessary and to refine spatial and temporal discretizations only where needed. A complete description of the overall strategy to efficiently control model and discretization errors up to a user-given tolerance is given in [4, 8]. In what follows, we will give a brief overview on the main ingredients.

3.1 Adaptive Network Simulation

For the discretization of the hyperbolic PDEs in the pipes, we apply an implicit box scheme [24], which reads for model (M3)

$$\frac{u_{i-1}^l + u_i^l}{2} = \frac{u_{i-1}^{l-1} + u_i^{l-1}}{2} - \frac{\Delta t}{\Delta x} (\mathbf{A}u_i^l + B(u_i^l) - \mathbf{A}u_{i-1}^l - B(u_{i-1}^l)) + \frac{\Delta t}{2} (g(u_{i-1}^l) + g(u_i^l)). \quad (11)$$

It uses step sizes Δx and Δt in space and time, respectively, and forms a system of nonlinear equations for the approximations $u_i^l \approx u(x_i, t_l)$. The scheme is closely related to the

finite difference method proposed in [21], where the midpoint rule is used to approximate the source term $g(u)$ – a fact we were not aware of until now. Explicit methods as recently presented in [9, 13] for large-scale natural gas pipeline networks can be an efficient alternative if the dynamics is not highly spread over the whole network. However, optimal control of compressor stations typically changes the dynamics close to the compressors in an unpredictable manner, which would force explicit integrators to apply very small time steps due to the well-known CFL condition. This effect can be even strengthened if the source term $g(u)$ becomes dominant in the turbulent region. So, we have decided to use an implicit scheme in order to choose an appropriate time step with respect to accuracy requirements only.

Dropping terms with B on the right-hand side yields a discretization for model (M2). No discretization for (M3) is necessary, since it can be solved analytically. The scheme is convergent of order two in space and order one in time. It is conservative and stable under mild conditions [24]. Each pipe of the network is discretized by using one of the three gas transport models described above and an individual step size in space, where both can vary over time. The global time steps taken by this scheme are also used for all algebraic model equations including model (M1). The adaptation of the discretization parameters $h := (\Delta x, \Delta t, (Mk)_{k \in \{1,2,3\}})$ is realized in a successive process of the classical loop

$$SOLVE \rightarrow ESTIMATE \rightarrow MARK \rightarrow REFINE. \quad (12)$$

Given all discretization parameters collected in h , the model equations are solved and error estimators are derived. These estimators are then used to mark pipes for spatial refinement or model enhancement and to adopt the global time step. The error estimators considered are based upon the discretized model equations and are supposed to measure the influence of the currently applied models and discretizations in each individual pipe on a generic user-defined output functional

$$M(u) = \int_Q N(u) d(x, t) + \sum_{v \in \mathcal{V}} \int_0^T N_v(u) dt + \sum_{i \in \mathcal{J} \setminus \mathcal{J}_{\text{PDE}}} \int_0^T N_i(u_i) dt. \quad (13)$$

Here, $Q = \Omega \times (0, T)$ with $\Omega = \bigcup_{j \in \mathcal{J}_{\text{PDE}}} [x_j^a, x_j^b]$ and the vector u_i is defined as $u_i(t) = (p(x_i^a, t), q(x_i^a, t), p(x_i^b, t), q(x_i^b, t))^T$ for all arcs $i \in \mathcal{J} \setminus \mathcal{J}_{\text{PDE}}$ that are modelled by algebraic equations. The functions $N(u)$, $N_v(u)$, and $N_i(u_i)$ define tracking-type costs on the respective sets (Ω , nodes, algebraic arcs) in the whole time interval $(0, T)$. In the spirit of dual weighted residual methods, the applied error estimators are computed via sensitivity information coming from adjoint equations of the discretized model equations [8]. Here, we will demonstrate their computation for the case that model (M2) is applied in all pipes. The adjoint equations of model (M2) with respect to $M(p, q)$ are given by

$$\begin{aligned} \xi_{1_t} + \frac{A}{\rho_0} \xi_{2_x} &= -\frac{\lambda \rho_0 c^2}{2DA} \frac{|q|q}{p^2} \xi_2 - N_p(p, q), \\ \xi_{2_t} + \frac{\rho_0 c^2}{A} \xi_{1_x} &= \frac{\lambda \rho_0 c^2}{DA} \frac{|q|}{p} \xi_2 - N_q(p, q), \end{aligned} \quad (14)$$

together with appropriate end, coupling, and node conditions, where also the functions N_v and N_i appear [3, 8]. The solution $\xi = (\xi_1, \xi_2)^T$ of the adjoint equations consists of the adjoint pressure and flow rate of the semilinear model (M2) with respect to the

functional $M(u)$. Let now $u = (p, q)^T$ be the solution of the nonlinear model (M1) and $u^h = (p^h, q^h)^T$ the approximate solution of the semilinear model (M2). Then, the difference between the functional $M(u)$ and $M(u^h)$ can be approximated using Taylor expansion, i.e., $M(u) - M(u^h) \approx M_p(u^h)(p - p^h) + M_q(u^h)(q - q^h)$. Eventually, the first derivatives M_p and M_q are replaced by using the adjoint system (14), which yields after a few calculations

$$M(u) - M(u^h) \approx \sum_{j \in \mathcal{J}_p} (\eta_{m,j}^{\text{LIN-NL}} + \eta_{t,j}^{\text{LIN}} + \eta_{x,j}^{\text{LIN}}) \quad (15)$$

with the a posteriori error estimators

$$\eta_{t,j}^{\text{LIN}} = \int_0^T \int_{x_j^a}^{x_j^b} -\xi^T (u_t^h - R_t(u^h)) \, dx \, dt, \quad (16a)$$

$$\eta_{x,j}^{\text{LIN}} = \int_0^T \int_{x_j^a}^{x_j^b} -\xi^T (\mathbf{A}u_x^h - R_x(\mathbf{A}u^h) - g(u^h) + R(g(u^h))) \, dx \, dt, \quad (16b)$$

$$\eta_{m,j}^{\text{LIN-NL}} = \int_0^T \int_{x_j^a}^{x_j^b} -\xi^T B(u^h)_x \, dx \, dt. \quad (16c)$$

Here, for the reconstruction operator R_t for the temporal derivative, we use central differences of order two, whereas R and R_x are defined by

$$R(u_i^h) = \frac{1}{16} \left(-u_{i-3/2}^h + 9u_{i-1/2}^h + 9u_{i+1/2}^h - u_{i+3/2}^h \right), \quad (17a)$$

$$R_x(u_i^h) = \frac{1}{24} \left(u_{i-3/2}^h - 27u_{i-1/2}^h + 27u_{i+1/2}^h - u_{i+3/2}^h \right), \quad (17b)$$

which gives fourth-order accuracy with function values $u_{i+j/2}^h$ at cell centers. The model error estimator $\eta_{m,j}^{\text{ALG-LIN}}$ between the algebraic and the semilinear model and the discretisation error estimators $\eta_{t,j}^{\text{NL}}$ and $\eta_{x,j}^{\text{NL}}$ for the nonlinear model are derived analogously for every pipe $j \in \mathcal{J}_p$; see [3, 8].

Based on this information, the following strategy to adapt the applied models as well as the discretization parameters is used [4]: First, the time interval $[0, T]$ is split into certain time blocks $[T_{k-1}, T_k]$ and the output functional (13), say M_k , and the error estimators (16), say $\eta_{m,j}^k, \eta_{t,j}^k, \eta_{x,j}^k$, are locally evaluated for the algebraic model and coarse meshes initially chosen. Second, models and discretization meshes are successively refined within the loop (12) until a user-prescribed tolerance **TOL** is achieved in the sense that

$$\frac{|M_k(u) - M_k(u^h)|}{|M_k(u^h)|} \approx \frac{|\sum_{j \in \mathcal{J}_p} (\eta_{m,j}^k + \eta_{t,j}^k + \eta_{x,j}^k)|}{|M_k(u^h)|} \leq \text{TOL}. \quad (18)$$

The problem of finding an optimal refinement strategy is a generalisation of the knapsack problem [4]. We apply a greedy-like strategy *maximum error-to-cost refinement* [4, Algorithm 3a] to keep the relative error below **TOL**, while retaining low computational costs. Third, once the solution meets the tolerance requirement in $[T_{k-1}, T_k]$, the models and discretisations are coarsened if appropriate, the simulation progresses to the next time interval, and the cycle repeats. The possible changes of the spatial discretizations between two time blocks is treated by a conservative projection, see [8, Sect. 6]. For further details on the computation of the error estimators and the adaptive strategy, we refer to [4, 6, 7, 8].

3.2 Gradient-Based Optimization Methods

The approach of a fully adaptive network simulation can be used to solve optimal control problems, where we consider objective functions of the generic form (13). We apply gradient-based optimization techniques, in particular the solver DONLP2 [33, 34], where a sequential quadratic programming with an active set strategy and only equality constrained subproblems is implemented. Since the computation of gradient information via difference quotients is rather inefficient, we apply a similar adjoint calculus as for the error estimators to get the necessary gradient information with respect to control variables of the respective optimization problem. The whole approach has been implemented in our in-house software package ANACONDA [23].

Let c be the vector of control variables defined by $(H_{ad}(t), \Delta p(t))$ at certain time points and $E(u^h, c) = 0$ the system of all nonlinear discretized model equations including initial, boundary and coupling conditions. Then, our goal is to solve the constrained optimal control problem

$$\text{Minimize}_{c \in C_{ad}} M(u^h, c) \tag{19a}$$

$$\text{subject to } E(u^h, c) = 0, \quad \text{where } h \text{ is chosen such that} \tag{19b}$$

$$\left| \sum_{j \in \mathcal{J}_p} (\eta_{m,j}^k + \eta_{t,j}^k + \eta_{x,j}^k) \right| \leq |M_k(u^h, c)| \cdot \text{TOL} \quad \text{for all } [T_{k-1}, T_k], \tag{19c}$$

where C_{ad} is the closed and convex set of admissible controls c and $M(u^h, c)$ is the output functional defined in (13), which can now also depend on the control. We would like to solve this problem with gradient-based optimization techniques. To get the necessary gradient information, we apply the same adjoint approach as described above for the error estimators. First, given a control $c \in C_{ad}$, we adaptively solve the model equations by a greedy-like refinement strategy such that the tolerance requirements are fulfilled with appropriate discretization parameters collected in h . We fix the discretization and solve the linear adjoint equations

$$\left(\frac{\partial}{\partial u^h} E(u^h, c) \right)^T \xi^h = - \left(\frac{\partial}{\partial u^h} M(u^h, c) \right)^T \tag{20}$$

for the adjoint variables ξ^h . Then, the total derivative of the objective $M(u^h, c)$ with respect to the control variables c reads

$$\frac{d}{dc} M(u^h, c) = \frac{\partial}{\partial c} M(u^h, c) + (\xi^h)^T \frac{\partial}{\partial c} E(u^h, c), \tag{21}$$

where we have used that $\partial_{u^h} E(u^h, c) \partial_c u^h = -\partial_c E(u^h, c)$. This gradient is passed to the solver DONLP2, which delivers an improved control vector. The iteration is stopped if a certain tolerance prescribed for DONLP2 is reached.

4 Adaptive Simulation of Large Gas Networks

As an example from real gas networks in Germany, we consider the network *GasLib-582* from gaslib.zib.de [32]. The network consists of 582 nodes (31 sources, 129 sinks, and

422 inner nodes). The nodes are connected through 278 pipes, 269 short pipes, 26 valves, 23 control valves, and 5 compressor stations, totalling 609 edges. Figure 1 shows the network where some selected nodes are indicated that we will refer to later on.

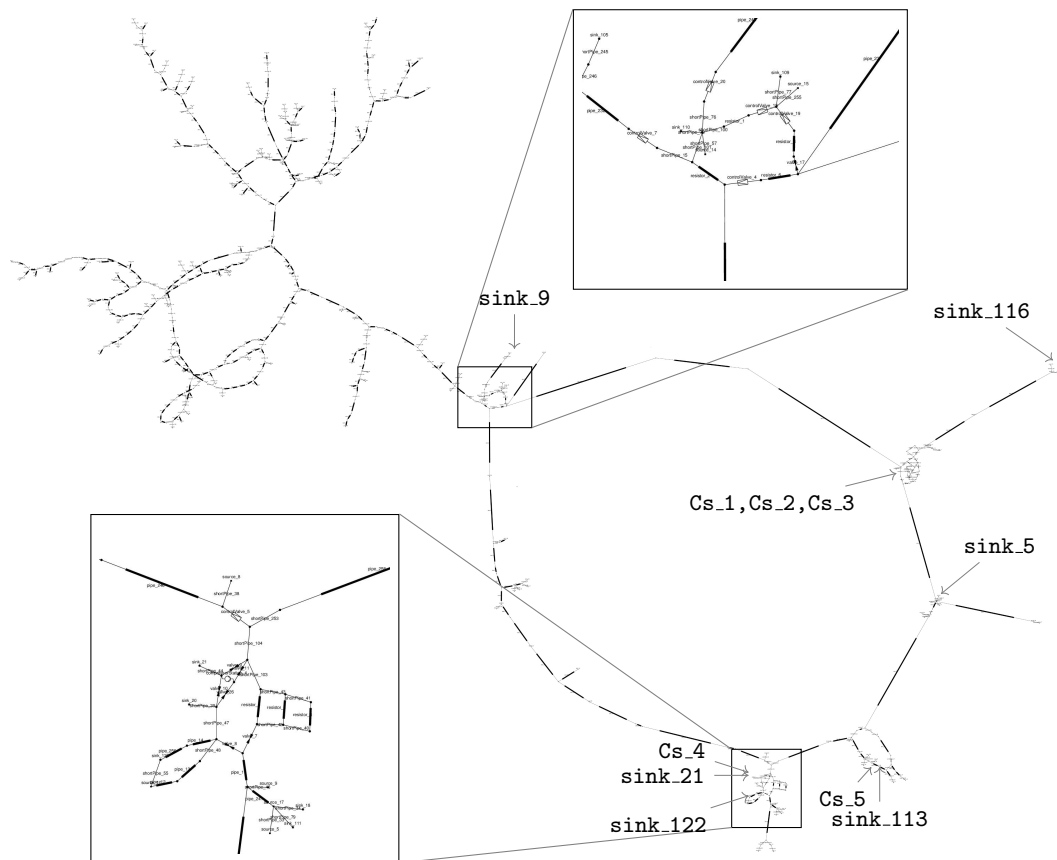


Figure 1: Topology of the large real-life gas network GasLib-582.

The settings of the network components with binary decisions are taken from a combined decision file originally provided by `gaslib.zib.de`. Initial data is generated by calculating a steady state solution for a given nomination (boundary data). For the simulation, the boundary data of some of the sinks (`sink_5`, `sink_9`, `sink_21`, `sink_113`, `sink_116`, `sink_122`) are taken time-dependent as well as the controls of the compressor stations, see Figures 2 and 3, respectively.

The adaptive simulations are run with tolerances ranging from 10^{-1} to 10^{-4} . Running the compressor stations needs a certain amount of energy and is relatively costly. Thus, one target is to run the network at minimal compressor costs. Also, consumers like big companies nominate a certain amount of gas and may additionally have some contractual agreements relating to the pressure of the gas provided. Hence, the aim is to fulfil these requirements in order to prevent contractual penalties. Having these examples in mind, we define the target functional to be given by the total energy consumption of the five compressor stations supplemented by the L^2 -norm of the difference between the actual pressure and a target

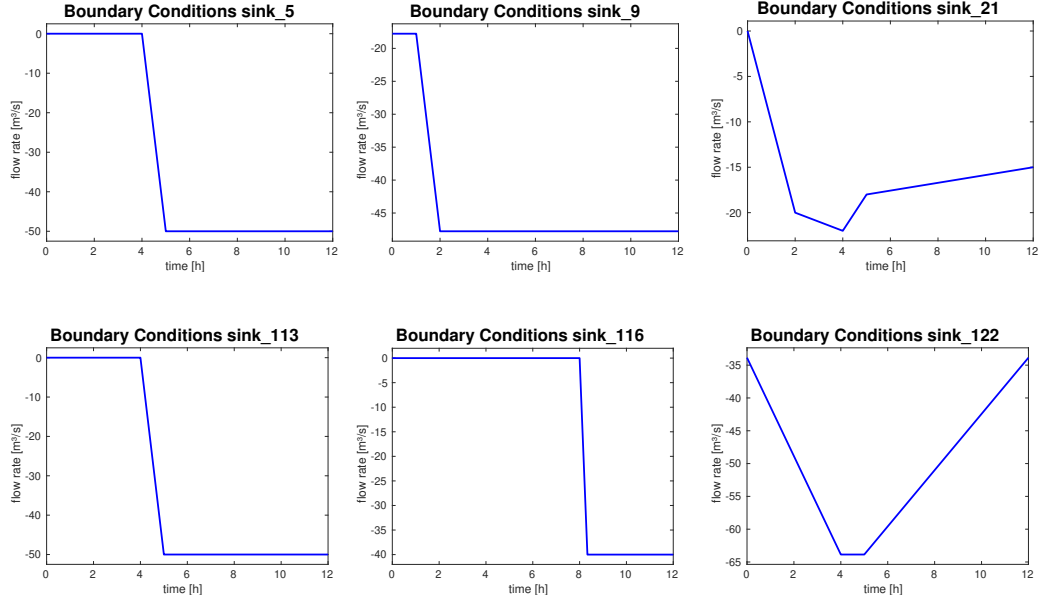


Figure 2: Time-dependent boundary conditions for sink 5, 9, 21, 113, 116, and 122.

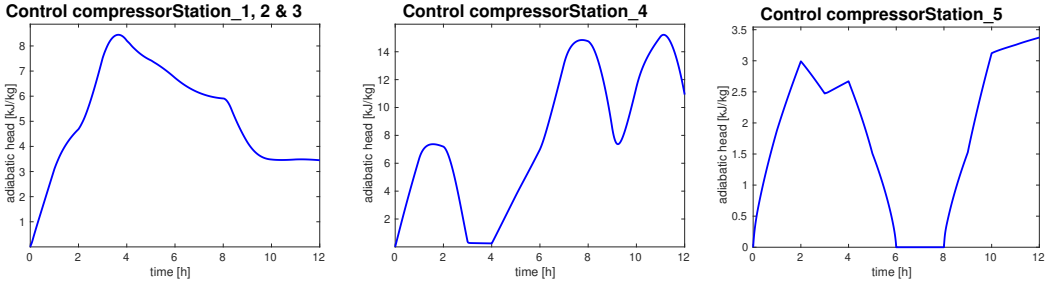


Figure 3: Time-dependent controls H_{ad} for compressors 1-5.

pressure at selected nodes. These are $S := \{\text{sink}_9, \text{sink}_{113}, \text{sink}_{116}, \text{sink}_{122}\}$, the location of which can be found in Figure 1. Thus, the objective function with appropriate weights reads

$$M(u) = 0.01 \cdot \sum_{cp \in \mathcal{J}_{cp}} \int_0^T P_{cp}(t) dt + \sum_{s \in S} \beta_s \int_0^T (p_s(t) - p_{s,target}(t))^2 dt, \quad (22)$$

where $\beta_s = (10^{-3}, 10^{-4}, 10^{-4}, 10^{-4})$ for $s = 9, 113, 116, 122$, respectively.

Table 1 shows the results for the model-space-time adaptive simulations. The relative error in the target functional $M(u^h)$ with respect to a reference solution, which is computed with $\Delta t = 20 s$ and a locally uniform spatial mesh size $\Delta x \leq 250 m$ adjusted to the pipe lengths, is presented. We observe that the error in the target functional decreases nicely with the given tolerance. Please note that the error estimators do not give a strict upper bound, but the quality of the error estimation is quite impressive for higher tolerances

Table 1: Simulation results for the large network GasLib-582

TOL	rel. error	$M(u_h)$	max/min Δt	max/min Δx	CPU [s]
5e-01	1.42e-02	837.82314	3600/1800	9936.87/255.061	7.06325
1e-01	1.42e-02	837.82314	3600/1800	9936.87/255.061	8.16174
5e-02	6.33e-03	831.29258	3600/1800	9936.87/255.061	9.46312
1e-02	3.94e-03	829.32319	3600/1800	9936.87/255.061	11.6008
5e-03	3.90e-03	829.28715	3600/1800	9936.87/255.061	10.8657
1e-03	2.68e-03	828.28308	1800/450	9936.87/255.061	41.4777
5e-04	7.54e-04	826.68920	450/450	9936.87/255.061	48.1188
1e-04	1.43e-04	826.18441	112.5/28.125	9936.87/255.061	358.386
reference solution		826.06608	20	249.984/204.049	533.596

[3, 8]. At the same time, the CPU time needed for computation of the simulation increases moderately with the tolerance going down. Please note that for the computation of the reference solution, no adjoint equations were solved nor have any error estimators been computed. We conclude that our fully adaptive algorithm is able to simulate a real-life gas network as GasLib-582 over a time horizon of 12 hours in a few seconds when, e.g., a practically sufficient tolerance 5×10^{-3} is requested.

Table 2: Usage of models in % for the large network

TOL	M_1	M_2	M_3
1e-01	100.0%	0.0%	0.0%
5e-02	95.8%	3.7%	0.5%
1e-02	89.9%	7.7%	2.3%
5e-03	89.1%	6.8%	4.1%
1e-03	60.2%	27.6%	12.2%
5e-04	41.2%	39.6%	19.1%
1e-04	15.1%	65.1%	19.8%

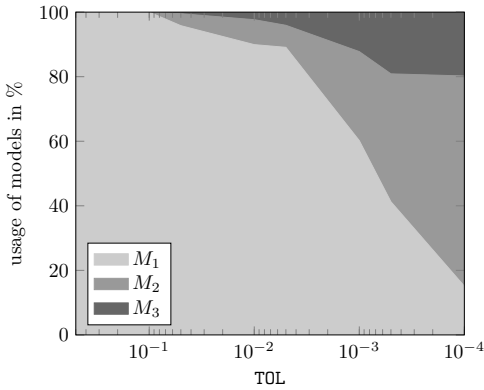


Figure 4: Usage of models in % for the simulation of the large network

Table 2 and Figure 4 illustrate which models are used to what extent during the simulations depending on the tolerance. Not surprisingly, the smaller the tolerance, the more detailed models are used by the adaptive algorithm.

We are also interested in where and when the model refinement takes place. For a tolerance $\text{TOL} = 10^{-3}$, we have selected a few pipes, which are adjacent to sinks in the network, see Figure 5. The first three pipes (p243, p256, p245) correspond to `sink_113`, `sink_122`, and `sink_9`, respectively. They all contribute to the target functional. The pipe p23 corresponds to `sink_5`, which is close to `sink_9`. The last two pipes (p233, p249) are away from any impact to the target functional. We clearly see that pipes adjacent or close to targets use more sophisticated models than remote pipes.

Another point of interest is how well the adaptive solution corresponds to the reference

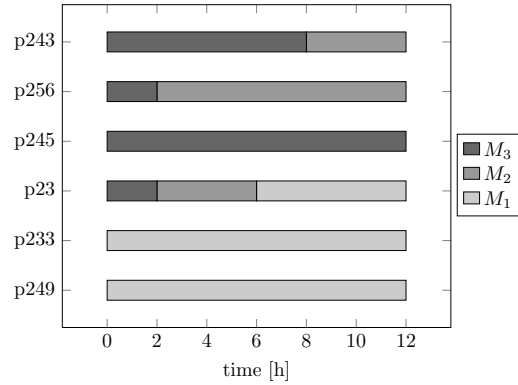


Figure 5: Models used over time for a selection of pipes.

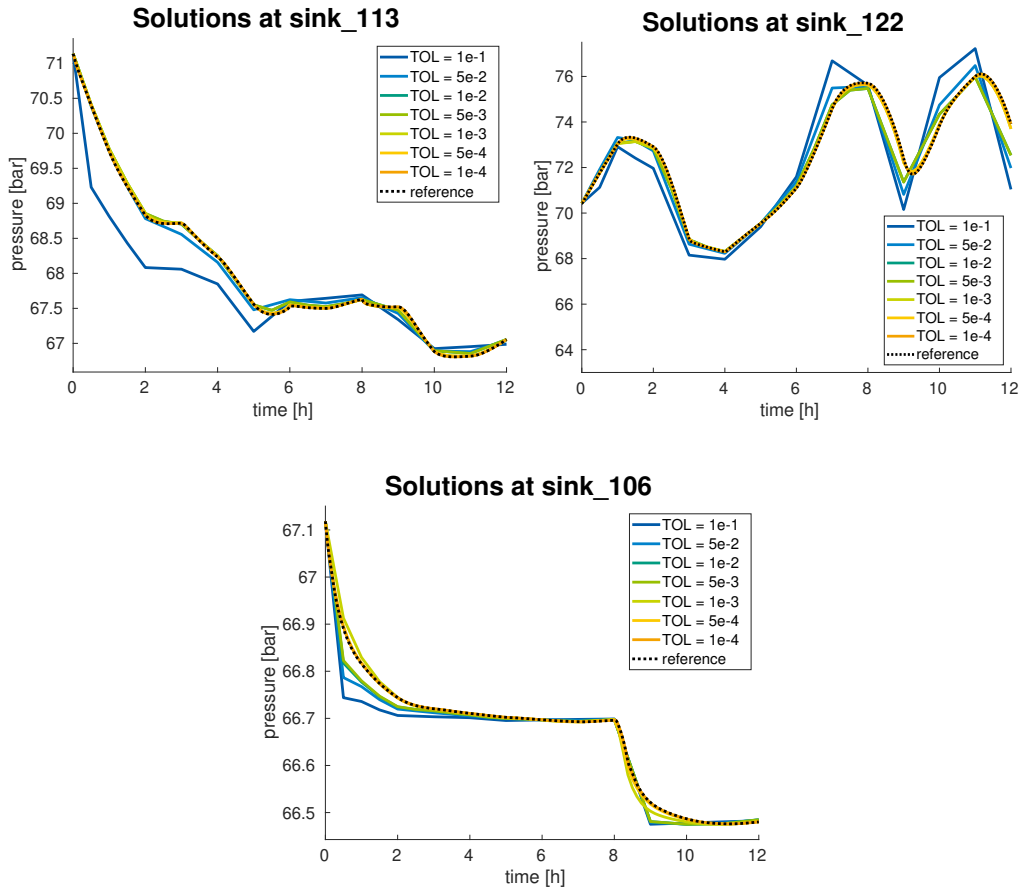


Figure 6: Adaptive solutions for different TOL at sinks `sink_113` and `sink_122` contributing to the target functional, and `sink_106` not contributing to the target functional.

solution. Figure 6 shows the pressure at `sink_113`, `sink_122`, and `sink_106` of the adaptive simulation using different values of TOL as well as the reference solution. It can be seen that for the sinks contributing to the target functional, i.e. `sink_113` and `sink_122`, the adaptive solution is quite close to the reference solution already for $\text{TOL} = 10^{-2}$ or 5×10^{-3} . For `sink_106`, this is the case for a tolerance of 10^{-3} or even lower.

5 Applications to Constrained Optimal Control

The operation of a gas network gives rise to various scenarios which can be treated by appropriate optimization tools. One important question in every day practice is concerned with the issue of nomination validation:

Given a stationary state A of the network, is it possible to reach a stationary state B satisfying certain constraints?

If the answer is yes, can we operate the network in an optimal, cost efficient way? Constraints under consideration can be lower and upper bounds on the pressure and the flow or the operating range of a compressor station. In what follows, we exemplarily apply methods from continuous optimization to answer these questions. A key point is an appropriate modelling of compressor stations, which is described next.

The physical model of a turbo compressor is determined by a characteristic field [35], see Figure 7a. A compressor station typically consists of multiple compressors that can be run in different configurations: single, serial, and parallel. Each configuration is again described by a characteristic field that overlap largely, see Figure 7b. Resulting from approximate convex decomposition [17, 26], we take an outer linear approximation of the physical model of the aggregated characteristic fields as a base, see Figure 7c. In order to make such a model applicable within an optimization, we approximate it by a semiconvex set K in the Q - H_{ad} -space, see Figure 7d. The approximation is semiconvex in the sense that for fixed H_{ad} , if $(Q_1, H_{ad}) \in K$ and $(Q_2, H_{ad}) \in K$, then

$$(\lambda Q_1 + (1 - \lambda)Q_2, H_{ad}) \in K \quad \forall \lambda \in [0, 1]. \quad (23)$$

The difference between the approximate convex decomposition model and the semiconvex approximation is displayed in Figure 7d. Property (23) allows to incorporate the characteristic diagram of a compressor station as a state constraint for the volumetric flow rate Q through it, see (26d) below. The pressure head H_{ad} is then only restricted by a flow-independent minimum and maximum value, $H_{ad,min}$ and $H_{ad,max}$, respectively.

The path from A to B mainly depends on the boundary values, especially the change of the flow rate q_s at the sinks. One could prescribe this change by a certain function in time, e.g. a linear one, over an appropriate time horizon and try to find a set of controls that guarantees the compliance of all operational restrictions. However, the identification of such transfer functions is often a difficult task. A second option, which we will follow here, is to relax the inflexibility of a fixed time-dependent boundary condition by considering the outflow rates q_s , $s \in \mathcal{J}_q$, as part of the controls and adding a weighted tracking type functional to the objective function, resulting in

$$M_{nv}(u, c) = \alpha \cdot \sum_{cp \in \mathcal{J}_{cp}} \int_0^T P_{cp}(t) dt + \sum_{s \in \mathcal{J}_q} \beta_s \int_0^T (q_s(t) - q_{s,target}(t))^2 dt. \quad (24)$$

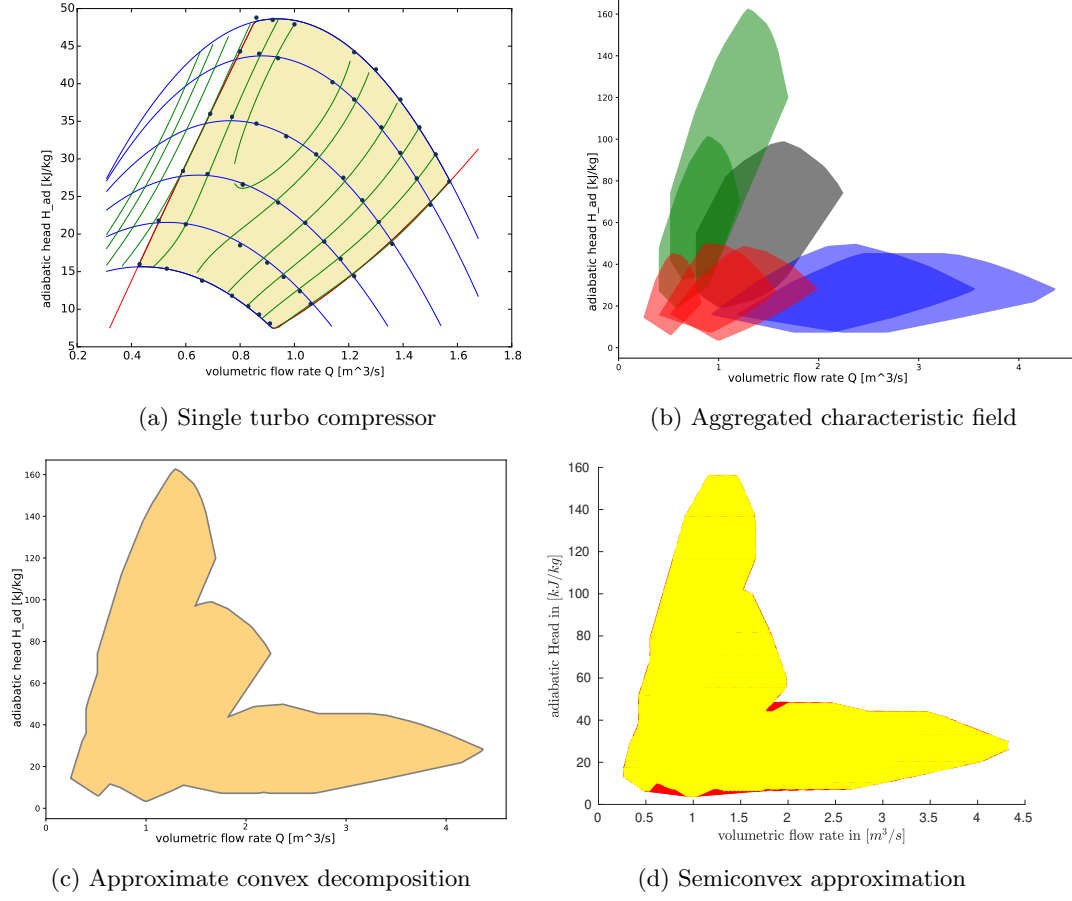


Figure 7: Modelling of compressor stations consisting of several single turbo compressors

with positive weights α , β_s , and $c = (\{H_{ad}^{cp}\}, \{q_s\})$ - the set of all pressure heads and outflow rates that have to be changed. It is beneficial that $q_{s,target}(t) = q_s^B$ for $t \in [T - t^*, T]$ for a sufficiently large $t^* < T$ and q_s^B being the desired new outflow rate at state B . The admissible set is defined as

$$C_{ad} := \{(H_{ad}^{cp}, q_s)_{cp \in \mathcal{J}_{cp}, s \in \mathcal{J}_q} : H_{ad,min}^{cp} \leq H_{ad}^{cp} \leq H_{ad,max}^{cp}, q_s \in \mathbb{R}\}. \quad (25)$$

We also consider lower and upper bounds for the flow rate q_s and the pressure p_s at certain sinks and sources with index sets \mathcal{J}_{pl} , \mathcal{J}_{pu} , \mathcal{J}_{ql} , and \mathcal{J}_{qu} , respectively. In general, $\mathcal{J}_{pl} \cap \mathcal{J}_{pu} \neq \emptyset$ and $\mathcal{J}_{ql} \cap \mathcal{J}_{qu} \neq \emptyset$.

Our resulting optimal control problem for the nomination validation reads as follows:

$$\text{Minimize}_{c \in C_{ad}} M_{nv}(u^h, c) \quad (26a)$$

$$\text{subject to } E(u^h, c) = 0, \quad \text{where } h \text{ is chosen such that} \quad (26b)$$

$$\left| \sum_{j \in \mathcal{J}_p} (\eta_{m,j}^k + \eta_{t,j}^k + \eta_{x,j}^k) \right| \leq |M_k(u^h, c)| \cdot \text{TOL} \quad \text{for all } [T_{k-1}, T_k], \quad (26c)$$

$$Q_{min}(H_{ad}^{cp}) \leq Q_{cp}^h \leq Q_{max}(H_{ad}^{cp}) \quad \text{for all } cp \in \mathcal{J}_{cp}, \quad (26d)$$

$$p_s^h(t_i) \geq p_s^l(t_i) \quad \text{for all discrete time points } t_i \text{ and } s \in \mathcal{J}_{pl}, \quad (26e)$$

$$p_s^h(t_i) \leq p_s^u(t_i) \quad \text{for all discrete time points } t_i \text{ and } s \in \mathcal{J}_{pu}, \quad (26f)$$

$$q_s^h(t_i) \geq q_s^l(t_i) \quad \text{for all discrete time points } t_i \text{ and } s \in \mathcal{J}_{ql}, \quad (26g)$$

$$q_s^h(t_i) \leq q_s^u(t_i) \quad \text{for all discrete time points } t_i \text{ and } s \in \mathcal{J}_{qu}. \quad (26h)$$

We apply the gradient-based SQP-solver DONLP2 [33, 34], which can handle control as well as state constraints of the form (26d)-(26h).

In the following sections, we show the applicability of the continuous optimization algorithm for nomination validation including the semiconvex approximation of the characteristic diagram as constraints for the compressor stations.

5.1 Network with Three Compressor Stations

For demonstration purpose, we firstly consider a simplified, but very illustrative network with three compressor stations, see Fig. 8.

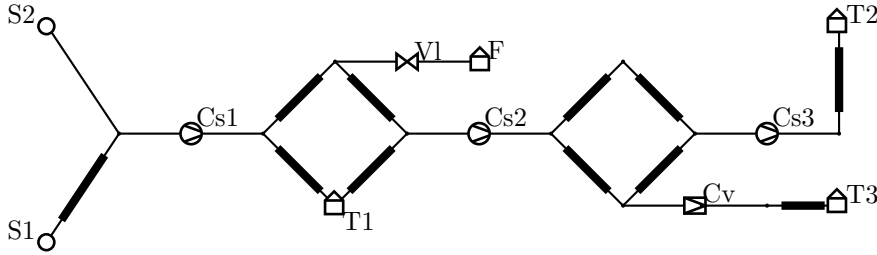


Figure 8: Network with three compressor stations

At time $t = 0$, the network is in a stationary state A , resulting from a simulation with stationary boundary conditions. The aim is to operate the network as to reach a stationary

state B under certain constraints. For the sinks T2 and T3, we have the following targets:

$$q_{T2,target}(t) = \begin{cases} 40 \text{ m}^3/\text{s}, & 0 \leq t < 7200 \text{ s}, \\ 5 \text{ m}^3/\text{s}^2 \cdot t + 30 \text{ m}^3/\text{s}, & 7200 \text{ s} \leq t < 21\,600 \text{ s}, \\ 60 \text{ m}^3/\text{s}, & 21\,600 \text{ s} \leq t \leq 43\,200 \text{ s}, \end{cases}$$

$$q_{T3,target}(t) = \begin{cases} 60 \text{ m}^3/\text{s}, & 0 \leq t < 7200 \text{ s}, \\ -5 \text{ m}^3/\text{s}^2 \cdot t + 70 \text{ m}^3/\text{s}, & 7200 \text{ s} \leq t < 21\,600 \text{ s}, \\ 40 \text{ m}^3/\text{s}, & 21\,600 \text{ s} \leq t \leq 43\,200 \text{ s}. \end{cases}$$

They enter the objective function in (24) with weights $\beta_{T2} = 10^{-4}$ and $\beta_{T3} = 10^{-5}$. The target state B has to be accessed under certain pressure constraints at T2 and T3,

$$\text{T2: } p \geq p_{T2}^l(t) \quad \text{with } p_{T2}^l(t) = \begin{cases} 79 \text{ bar} + 4/3 \text{ bar/h} \cdot t & 0 \leq t < 3 \text{ h}, \\ 83 \text{ bar} & 3 \text{ h} \leq t \leq 12 \text{ h}, \end{cases}$$

$$\text{T3: } p_{T3}^u \geq p \geq p_{T3}^l \quad \text{with } p_{T3}^u = 61 \text{ bar}, p_{T3}^l = 59 \text{ bar}.$$

The constraints for the compressor stations Cs1-Cs3 are given by identical characteristic fields as shown in Fig. 10. We choose $\alpha = 0.1$ as weight in (24).

The simulation interval is [0 h,12 h]. The discrete control vector $c \in \mathbb{R}^{240}$ consists of the three adiabatic heads $H_{ad}^{Csk}(t_i)$, $k = 1, 2, 3$, of the compressor stations and the flow rates $q_{Tk}(t_i)$, $k = 2, 3$, taken at the discrete control points $t_i = i \cdot 900 \text{ s}$, $i = 1, \dots, 48$. We use linear interpolation between the control points whenever necessary. The optimization algorithm DONLP2 equipped with gradient information delivers solutions for tolerance $\text{TOL} = 5 \times 10^{-4}$ after 16.5 min computing time. The corresponding targets and constraints of the sinks T2 and T3 are shown in Figure 9. We nicely see that the targets $q_{T2,target}(t)$ and $q_{T3,target}(t)$ are met very well by the control variables $q_{T2}(t)$ and $q_{T3}(t)$ during the optimization process and that also the constraints on the pressures $p_{T2}(t)$ and $p_{T3}(t)$ at the sinks are maintained.

The compressor stations are controlled via their individual adiabatic heads. These controls are shown in Figure 10. On the left hand side, the controls are drawn inside the characteristic field. We see that the controls stay inside the characteristic field and thus meet the technical constraints of the compressor stations.

Eventually, we would like to mention that relaxing the tolerance of DONLP2 to $\text{TOL} = 5 \times 10^{-3}$ still yields satisfactory results after 7.5 min computing time, but the solutions found are less smooth.

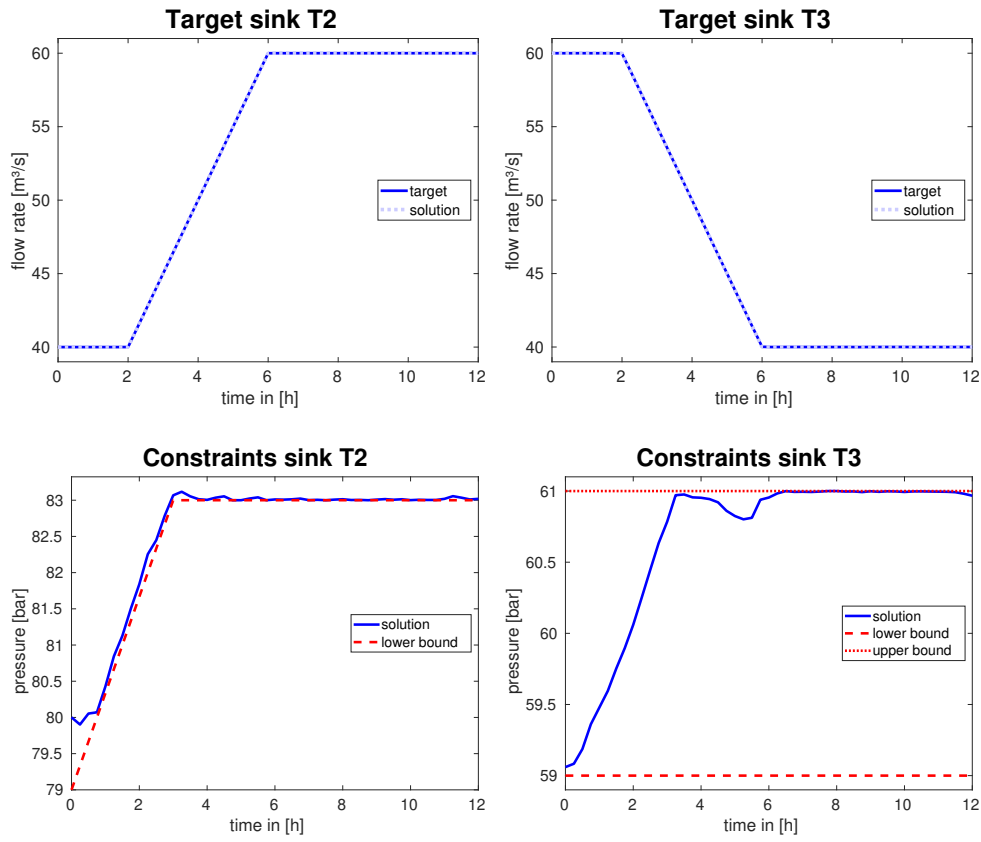


Figure 9: Controlled flow rate $q_s(t)$ (top) and pressure $p_s(t)$ (bottom) compared to target values $q_{s,target}(t)$ and constraints $p_s^{l,u}(t)$ for sinks $s=T2, T3$

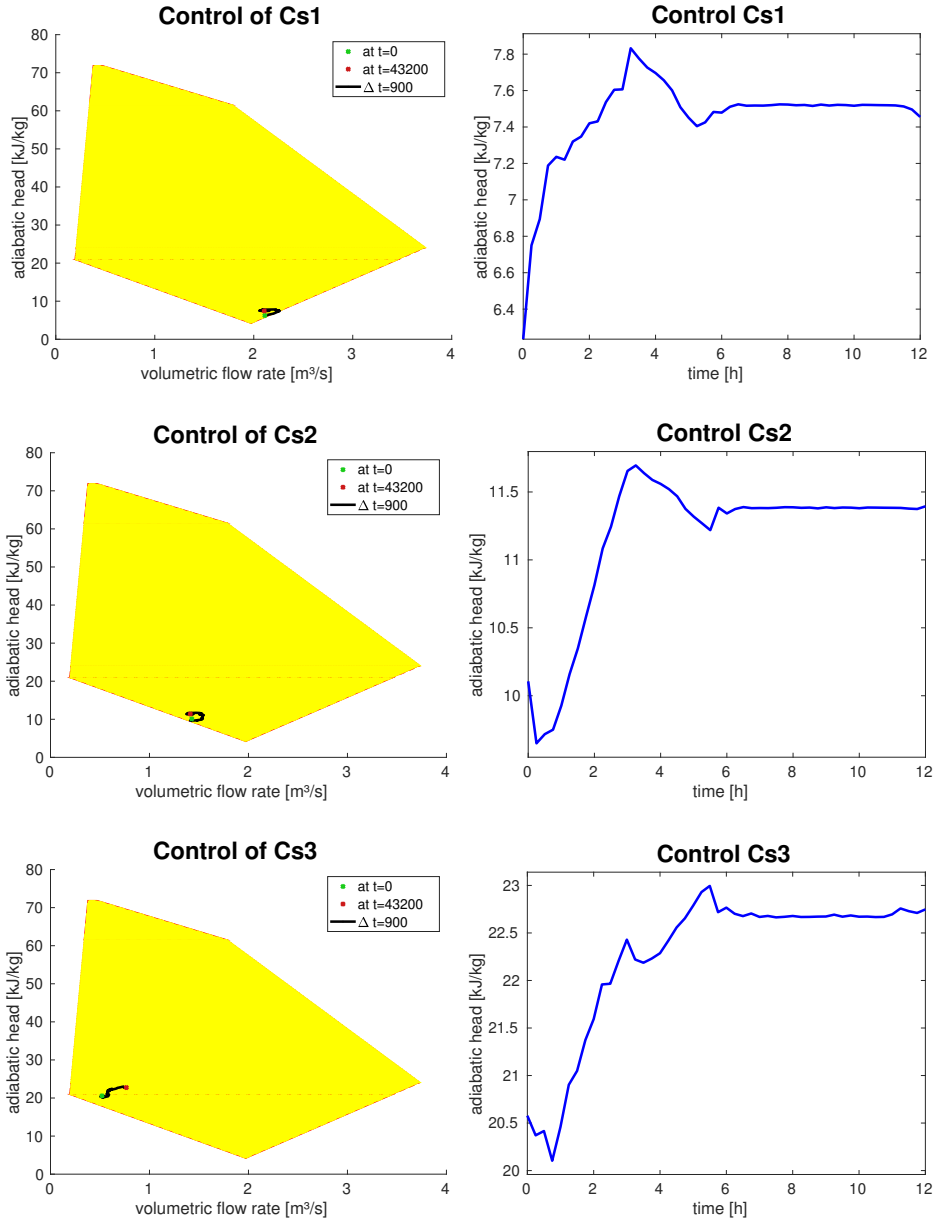


Figure 10: Controls $H_{ad}^{cp}(t)$ and constraints given by the (Q, H_{ad}) -diagrams of the compressor stations $cp=Cs1, Cs2, Cs3$ (top to bottom)

5.2 The Greek Network (GasLib-134)

As second example, we consider the real Greek network with 134 nodes including 3 sources, 45 sinks as well as 133 edges, one compressor station and one control valve, see Fig. 11. The specific data are available from gaslib.zib.de.

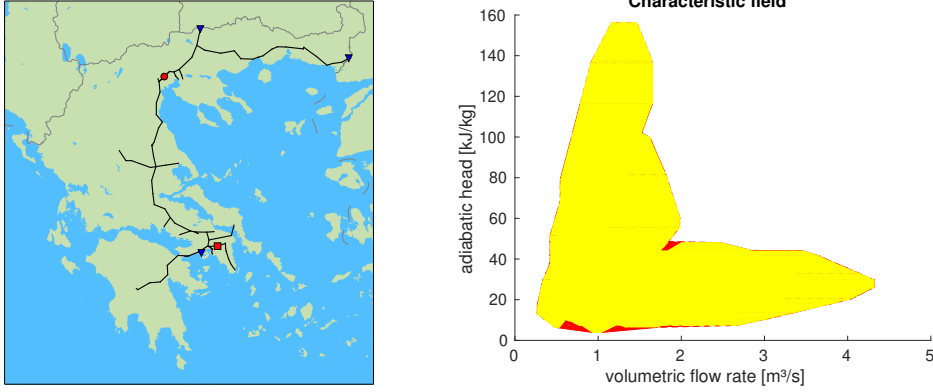


Figure 11: The Greek network (GasLib-134), reproduced from gaslib.zib.de (left), and characteristic field of the compressor station `cs` (right).

Table 3: Simulation results for the Greek network GasLib-134

TOL	rel. error	$M(u_h)$	max/min Δt	max/min Δx	M1:M2:M3 [%]	CPU [s]
1e-01	6.66e-03	0.0903765	7200/3600	18297.5/162.835	69:31:00	0.754
1e-02	1.27e-03	0.0898926	7200/3600	18297.5/162.835	43:57:00	0.907
1e-03	4.41e-04	0.0898186	1800/900	18297.5/162.835	14:84:02	3.387
1e-04	6.71e-05	0.0897850	225/225	18297.5/162.835	08:81:11	14.74
1e-05	2.36e-06	0.0897788	225/14.0625	18297.5/162.835	04:73:23	104.7
reference solution		0.0897790	10	250/162.835	0:0:100	1273

First, we check typical simulation results for a given control for the compressor station and varying tolerances. Exemplary results for $T = 24$ h are presented in Tab. 3. Practically sufficient accuracy is achieved with $\text{TOL} = 10^{-2}$.

Second, we are again interested in computing an optimized way to transfer the gas network from a stationary state A to another stationary state B under certain constraints. Except one, all sinks and sources have the same structure for the target functional:

$$q_{s,target}(t) = \begin{cases} q_s^A, & 0 \leq t < t_1, \\ q_s^A + \frac{t-t_1}{t_2-t_1} (q_s^B - q_s^A), & t_1 \leq t < t_2, \\ q_s^B, & t_2 \leq t \leq T. \end{cases}$$

for $s = 1, \dots, 47$, and with $t_1 = 2$ h, $t_2 = 6$ h, and simulation time $T = 24$ h. At source `node_20`, which can be identified to be the small blue triangle in the very north of Greece in

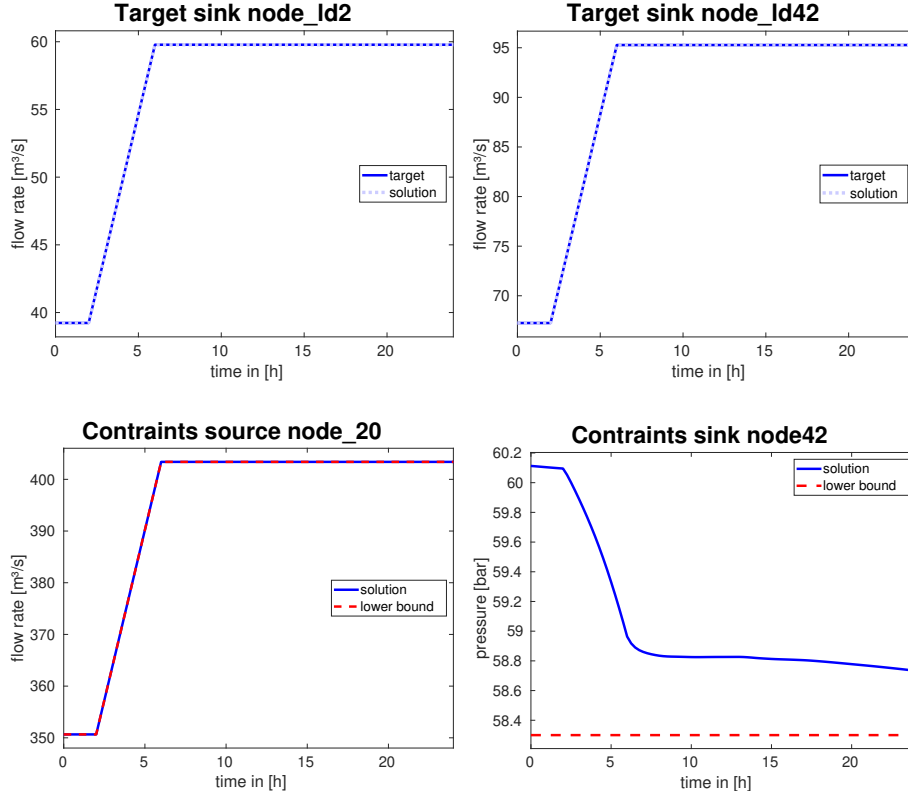


Figure 12: Controlled flow rates $q_s(t)$ compared to target values $q_{s,target}(t)$ for $s = 2, 42$ (top), flow rate $q_{20}(t)$ and pressure $p_{42}(t)$ compared to constraints q_{20}^l and p_{42}^l (bottom) for discrete control points with $\Delta t = 900$ s

Figure 11, we prescribe the pressure in order to get a well-defined stationary state. We set

$$p_{20}(t) = \begin{cases} p_{20}^A & 0 \leq t < t_1, \\ p_{20}^A + \frac{t-t_1}{t_2-t_1} (p_{20}^B - p_{20}^A) & t_1 \leq t < t_2, \\ p_{20}^B & t_2 \leq t \leq T. \end{cases}$$

In order to achieve the stationary state B in the end, we set the lower bound for the flow rate at source `node_20` to be

$$q_{20}^l(t) = \begin{cases} q_{20}^A & 0 \leq t < t_1, \\ q_{20}^A + \frac{t-t_1}{t_2-t_1} (q_{20}^B - q_{20}^A) & t_1 \leq t < t_2, \\ q_{20}^B & t_2 \leq t \leq T. \end{cases}$$

Further constraints are defined for the sinks `node_42` and `node_45`,

$$p_{42}(t) \geq p_{42}^l = 58.3 \text{ bar} \quad \text{and} \quad p_{45}(t) \geq p_{45}^l = 61 \text{ bar}.$$

They are located in the very south and south-west of the network, respectively. The constraints for the compressor station `cs` is given by a characteristic field as shown in Fig. 11.

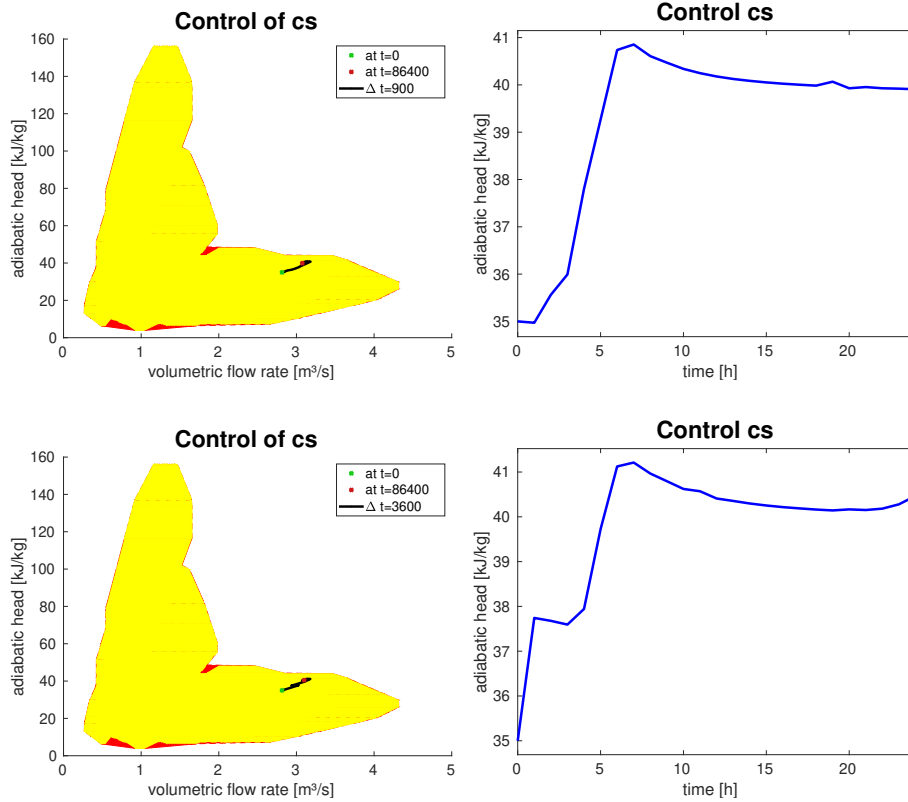


Figure 13: Control $H_{ad}^{cs}(t)$ and constraints given by the (Q, H_{ad}) -diagram of the compressor station cs for discrete control points with $\Delta t = 900$ s (top) and $\Delta t = 3600$ s (bottom)

We employ the semiconvex approximation of the polyhedral approximation as described above, see Fig. 7d.

The simulation interval is now $[0 \text{ h}, 24 \text{ h}]$. Beside the adiabatic head $H_{ad}^{cs}(t_i)$ for the compressor station, we consider all flow rates $q_s(t_i)$, $s = 1, \dots, 47$, at the discrete control points $t_i = i 900 \text{ s}$, $i = 1, \dots, 96$ as control variables, which gives $c \in \mathbb{R}^{4608}$. As a consequence, we enforce $\Delta t \leq 900 \text{ s}$ in our simulations to reach every control point with our adaptive scheme. We further set $\beta_s = 10^{-5}$ for all s and $\alpha = 1$ in the objective function (24). The optimization is challenging due to the additional state constraints. It was run with DONLP2 with a tolerance $\text{TOL} = 10^{-3}$ and took 10.1 min. We note that the dimension of the overall discrete state vector taken over space and time reaches more than a million in certain cases. Fig. 12 shows exemplary results for the targets of two selected nodes. The variable operation mode for the compressor station is plotted in Fig. 13 (top). All constraints are satisfied.

We have also reduced the discrete control points to $t_i = i 3600 \text{ s}$, $i = 1, \dots, 24$, which scales down the dimension of the control space to $c \in \mathbb{R}^{1152}$. DONLP2 was still able to find a feasible solution after 2.5 min. The corresponding operation mode for the compressor station is shown in Fig. 13 (bottom). It differs from the solution found for $\Delta t = 900 \text{ s}$.

6 Conclusion and Outlook

We have presented a novel optimization approach to support a transient management of large-scale gas networks with real semiconvex models for aggregated characteristic fields of compressor stations. Given the significantly reduced computational time for a one-time simulation by fully self-adaptive space-time-model discretizations and the associated inherent error control, the method proposed is a promising candidate for a reliable work horse in a predictive transient software framework that creates gas flow schedules and forecasts in near real-time. As an example, we have studied the practically important issue of nomination validations, i.e., transferring the gas network from a stationary state to another stationary state usually described by a change in the gas demands by consumers. During this process certain state constraints have to be satisfied, making the corresponding optimal control problem challenging. We could observe that treating the new outflow rates as control variables and adding regularization terms of tracking type for them to the objective function is an attractive way to find answers to the question whether a desired steady state can be reached.

In future projects, we will include mixed integer formulations to represent network topology changes and use probabilistic constraint optimization to investigate the influence of uncertainties.

Declarations

Funding. The authors P. Domschke and J. Lang are supported by the Deutsche Forschungsgemeinschaft (DFG, German Research Foundation) within the collaborative research center TRR154 “Mathematical modeling, simulation and optimisation using the example of gas networks“ (Project-ID239904186, TRR154/2-2018, TP B01).

Conflicts of interest/Competing interests. The authors declare that they have no known competing financial interests or personal relationships that could have appeared to influence the work reported in this paper.

Availability of data and material. Detailed descriptions of the gas networks GasLib-582 and GasLib-134 can be found at gaslib.zib.de.

Code availability. The nonlinear programming package DONLP2 by Peter Spellucci is free for academic use only, commercial use needs licensing.

References

- [1] A. Beylin, A.M. Rudkevich, and A. Zlotnik. Fast transient optimization of gas pipelines by analytic transformation to linear programs. In *PSIG Annual Meeting, 5-8 May 2020*. Pipeline Simulation Interest Group, PSIG-2003, 2020.
- [2] R. Burlacu, H. Egger, M. Gross, A. Martin and M.E. Pfetsch, L. Schewe, M. Sirvent, and M. Skutella. Maximizing the storage capacity of gas networks: a global MINLP approach. *Optimization and Engineering*, 20:543–573, 2019.

- [3] P. Domschke. *Adjoint-Based Control of Model and Discretization Errors for Gas Transport in Networked Pipelines*. PhD thesis, TU Darmstadt, 2011.
- [4] P. Domschke, A. Dua, J. J. Stolwijk, J. Lang, and V. Mehrmann. Adaptive refinement strategies for the simulation of gas flow in networks using a model hierarchy. *Electronic Transactions on Numerical Analysis*, 48:97–113, 2018.
- [5] P. Domschke, B. Geißler, O. Kolb, J. Lang, A. Martin, and A. Morsi. Combination of nonlinear and linear optimization of transient gas networks. *INFORMS J. Comput.*, 23:605–617, 2011.
- [6] P. Domschke, O. Kolb, and J. Lang. Adjoint-based control of model and discretisation errors for gas flow in networks. *Int. J. Math. Model. Numer. Optim.*, 2:175–193, 2011.
- [7] P. Domschke, O. Kolb, and J. Lang. Adjoint-based control of model and discretization errors for gas and water supply networks. In S. Koziel and X.-S. Yang, editors, *Computational Optimization and Applications in Engineering and Industry*, volume 359 of *Studies in Computational Intelligence*, pages 1–18. Springer, 2011.
- [8] P. Domschke, O. Kolb, and J. Lang. Adjoint-based error control for the simulation and optimization of gas and water supply networks. *Applied Mathematics and Computation*, 259:1612–1634, 2015.
- [9] S.A. Dyachenko, A. Zlotnik, A.O. Korotkevich, and M. Chertkov. Operator splitting method for simulation of dynamic flows in natural gas pipeline networks. *Physical D*, 361:1–11, 2017.
- [10] H. Egger. A robust conservative mixed finite element method for isentropic compressible flow on pipe networks. *SIAM Journal on Scientific Computing*, 40:A108–A129, 2018.
- [11] K. Ehrhardt and M.C. Steinbach. Nonlinear optimization in gas networks. In Hans G. Bock, Ekaterina A. Kostina, Hoang X. Phu, and Rolf Ranacher, editors, *Modeling, Simulation and Optimization of Complex Processes*, pages 139–148. Springer, 2005.
- [12] S. Grundel, N. Hornung, B. Klaassen, P. Benner, and T. Clees. Computing surrogates for gas network simulation using model order reduction. In S. Koziel and L. Leifsson, editors, *Surrogate-Based Modeling and Optimization*, pages 189–212. Springer, New York, NY, 2013.
- [13] V. Gyrya and A. Zlotnik. An explicit staggered-grid method for numerical simulation of large-scale natural gas pipeline networks. *Applied Mathematical Modelling*, 65:34–51, 2019.
- [14] M. Hahn, S. Leyffer, and V. Zavala. Mixed-integer pde-constrained optimal control of gas networks. Technical Report ANL/MCS-P7095-0817, Argonne National Laboratory, 2017.
- [15] F.M. Hante, G. Leugering, A. Martin, L. Schewe, and M. Schmidt. *Industrial Mathematics and Complex Systems: Emerging Mathematical Models, Methods and Algorithms*, chapter Challenges in Optimal Control Problems for Gas and Fluid Flow in Networks of Pipes and Canals: From Modeling to Industrial Applications, pages 77–122. Springer Singapore, Singapore, 2017.

- [16] M. Herty. Modeling, simulation and optimization of gas networks with compressors. *Netw. Heterog. Media*, 2:81–97, 2007.
- [17] B. Hiller and T. Walther. Improving branching for disjunctive polyhedral models using approximate convex decompositions. Report 17-68, Zuse-Institut Berlin (ZIB), November 2017.
- [18] IEA. The Role of Gas in Today’s Energy Transitions. Technical report, Paris, <https://www.iea.org/reports/the-role-of-gas-in-todays-energy-transitions>, 2019.
- [19] J. Jalving, Y. Cao, and M. Zavala. Graph-based modeling and simulation of complex systems. *Computers & Chemical Engineering*, 125:134–154, 2019.
- [20] J. Jalving and V.M. Zavala. An optimization-based state estimation framework for large-scale natural gas networks. *Ind. Eng. Chem. Res.*, 57:5966–5979, 2018.
- [21] T. Kiuchi. An implicit method for transient gas flows in pipe networks. *International Journal of Heat and Fluid Flow*, 15(5):378–383, 1994.
- [22] T. Koch, B. Hiller, M.E. Pfetsch, and L. Schewe, editors. *Evaluating Gas Network Capacities*. MOS-SIAM Series on Optimization. SIAM, 2015.
- [23] O. Kolb. *Simulation and Optimization of Gas and Water Supply Networks*. PhD thesis, TU Darmstadt, 2011.
- [24] O. Kolb, J. Lang, and P. Bales. An implicit box scheme for subsonic compressible flow with dissipative source term. *Numer. Algorithms*, 53:293–307, 2010.
- [25] J. Lang and P. Mindt. Entropy-preserving coupling conditions for one-dimensional Euler systems at junctions. *Networks & Heterogeneous Media*, 13:177–190, 2018.
- [26] J.-M. Lien and N.M. Amato. Approximate convex decomposition of polygons. *Computational Geometry*, 35:100–123, August 2006.
- [27] D. Mahlke, A. Martin, and S. Moritz. A mixed integer approach for time-dependent gas network optimization. *Optim. Methods Softw.*, 25:625–644, 2010.
- [28] T.W.K. Mak, P.V. Hentenryck, A. Zlotnik, and R. Bent. Dynamic compressor optimization in natural gas pipeline systems. *INFORMS Journal on Computing*, 31:40–65, 2019.
- [29] P. Mindt, J. Lang, and P. Domschke. Entropy-preserving coupling of hierarchical gas models. *SIAM Journal on Mathematical Analysis*, 51:4754–4775, 2019.
- [30] M.E. Pfetsch, A. Fügenschuh, B. Geißler, N. Geißler, R. Gollmer, B. Hiller, J. Humpola, T. Koch, T. Lehmann, A. Martin, A. Morsi, J. Rövekamp, L. Schewe, M. Schmidt, R. Schultz, R. Schwarz, J. Schweiger, C. Stangl, M.C. Steinbach, S. Vigerske, and B.M. Willert. Validation of nominations in gas network optimization: models, methods, and solutions. *Optimization Methods and Software*, 30:15–53, March 2014.
- [31] D. Rose, M. Schmidt, M.C. Steinbach, and B.M. Willert. Computational optimization of gas compressor stations: Minlp models versus continuous reformulations. *Mathematical Methods of Operations Research*, 83:409–444, Jun 2016.

- [32] M. Schmidt, D. Aßmann, R. Burlacu, J. Humpola, I. Joormann, N. Kanelakis, T. Koch, D. Oucherif, M.E. Pfetsch, L. Schewe, R. Schwarz, and M. Sirvent. GasLib – A Library of Gas Network Instances. *Data*, 2:article 40, 2017.
- [33] P. Spellucci. A new technique for inconsistent QP problems in the SQP method. *Mathematical Methods of Operations Research*, 47:355–400, 1998.
- [34] P. Spellucci. An SQP method for general nonlinear programs using only equality constrained subproblems. *Mathematical Programming*, 82:413–448, 1998.
- [35] T. Walther and B. Hiller. Modelling compressor stations in gas networks. Report 17-67, Zuse-Institut Berlin (ZIB), November 2017.
- [36] A. Zlotnik, K. Sundar, A.M. Rudkevich, A. Beylin, and X. Li. Optimal control for scheduling and pricing intra-day natural gas transport on pipeline networks. In *2019 IEEE 58th Conference on Decision and Control (CD)*, 2019. Palais des Congrès et des Expositions Nice AcropolisNice, France, December 11-13, 2019.